THE JOURNAL OF PHYSICAL CHEMISTRY A

Article

pubs.acs.org/JPCA

Dissipative Dynamics of Two-Level Systems in Low Temperature Glasses

Ke-Wei Sun[†,‡] and Yang Zhao*[,‡]

[†]School of Science, Hangzhou Dianzi University, Hangzhou 310018, China

[‡]Division of Materials Science, Nanyang Technological University, 50 Nanyang Avenue, Singapore 639798

ABSTRACT: An approach based on a non-Markovian time-convolutionless polaron master equation is used to probe dynamics of a central chromophore embedded in a bath of two-level systems commonly found in low-temperature glasses. By treating the Hamiltonian in the polaron frame, we can account for initial nonequilibrium bath states as well as the spatially correlated environmental effect. Relevant realistic situations are explored by adopting parameters from previous experiments. It is found that the temperature of the boson bath has a substantial effect on the population relaxation and the decoherence process, and a higher temperature also results in a higher saturation value of the entanglement entropy, while the coupling between the chromophore and the TLS has an effect that goes counter to that of the temperature.

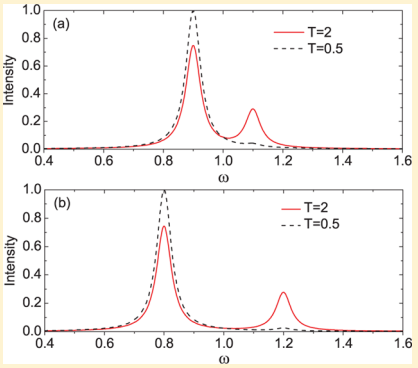

I. INTRODUCTION

Observations of glasses at low temperatures point to the presence of additional degrees of freedom, as compared to crystals with similar compositions. This additional freedom leads to higher specific heat, enhanced ultrasound attenuation, and various other anomalies.[1,2] It was soon realized that those degrees of freedom saturate at high microwave or acoustic power, and are not associated with vibrations. For very low temperatures, only the two lowest energy levels of a double minimum potential need be considered. Consequently, the complex dynamics of glasses can be reduced to a random array of two-level systems (TLSs).[3−10] As a simple, phenomenological description, the model of TLSs was very successful in helping understand various anomalies in glasses.

A number of low-temperature single molecule spectroscopy (SMS) studies on chromophores embedded in organic glasses have led to the observations of a wide range of spectral behaviors.[11−15] The presence of spectral diffusion, a phenomenon of peak absorption frequency movements in successive measurements on chromophores, is detected by hole-burning spectroscopy (HB) and three-pulse photon echo (3PE) experiments.[16−19] In addition, the absorption spectrum of a dilute collection of chromophores in glass is usually inhomogeneously broadened,[5,20−22] reflecting the extent to which the solvent environments differ, and hence is related to the local disorder around the chromophore. TLS flips due to tunneling will also modulate the transition frequency of the chromophore. Generally, line shapes show a surprising variation and, in some circumstances, single chromophores are known to produce multiplets of lines.[5]

It is commonly believed that the fluctuations of a low-temperature amorphous system can be described by the dynamics of the TLSs that are coupled to the chromophores via phonon fields. In addition, the TLS concentration in glasses is almost independent of the chemical nature of the glass. At a few Kelvins, it turns out that a single chromophore has less than one TLS in its immediate vicinity with coupling sufficiently strong to give rise to spectral diffusion of the chromophore.[11] Therefore, for simplicity, we start with a model describing a single TLS and a chromophore under the influence of a boson bath.

As in the aforementioned chromophore−TLS system, energy scales for vibronic relaxation and spin−phonon coupling are comparable, and the system can be considered in an intermediate coupling regime, where the traditional second-order perturbation approach is inaccurate.[23−25] This leads to dynamics studies using nonperturbative approaches,[26−29] such as numerically exact iterative path integral methods,[30−35] sophisticated stochastic treatments of the system−bath models,[36] and hierarchical equation of motion approach.[37−40] However, computationally intensive nonperturbative methods always become inefficient as the system size is large or when there are multiple excitations. Recently, the non-Markovian time-convolutionless (TCL) polaron master equation, capable of interpolating between weak and strong spin−phonon coupling regimes and handling initial nonequilibrium bath states and spatially correlated environments, has been employed to describe excitation dynamics in multichromophoric systems,[25,41−44] and in particular, this approach is used to treat an extension of the conventional spin−boson model to include an additional spin bath.[8] In this work, we investigate the dynamics of two coupled pseudospins in contact with a non-Markovian dissipative bath. The temperature effect on the von Neumann entropy of the

Received: January 3, 2014
Revised: February 24, 2014
Published: February 28, 2014

dx.doi.org/10.1021/jp5000717 | J. Phys. Chem. A 2014, 118, 2220−2227

system (chromophore+TLS) is also studied. The linear absorption spectrum of the chromophore is calculated based on the experimental parameters set for terylene in polystyrene.

The remainder of this paper is organized as follows. In Section II, the model and the method are presented. The dynamics of the system and the absorption spectra are studied in Section III. Conclusions are drawn in Section IV.

II. MODEL SYSTEM AND METHODOLOGY

We consider a model describing a chromophore and a single TLS both coupled to a common strain field of the glassy medium. The Hamiltonian can be written as[3,5,45]

$$\tilde{\mathcal{H}} = \frac{\omega_0}{2}\sigma_{z0} + \frac{\varepsilon}{2}\sigma_{z1} - \frac{\Delta}{2}\sigma_{x1} + H_B + \sum_k f_k(b_k + b_k^\dagger)\sigma_{z0} + \sum_k g_k(b_k + b_k^\dagger)\sigma_{z1} \tag{1}$$

Here, the chromophore Hamiltonian has been truncated to that of a pseudospin with $s = 1/2$, assuming that the experiments are carried near resonance with the optical transition of frequency ω_0. The 0 subindex refers to the chromophore, and the 1 subindex to the TLS with asymmetry ε and tunneling matrix element Δ. $H_B = \Sigma_k \omega_k b_k^\dagger b_k$ represents the Hamiltonian for the boson bath, where $b_k^\dagger(b_k)$ corresponds to the creation (annihilation) operator of the kth mode of the phonon bath, with frequency ω_k. We have also introduced coefficients f_k (g_k) to represent the coupling of the chromophore (TLS) to the bath mode k. Transformation of the Hamiltonian (1) via a unitary operator

$$U = \exp\left\{-\sum_q \frac{f_k}{\omega_k}(b_k^\dagger - b_k)\sigma_{z0}\right\} \tag{2}$$

yields a dressed Hamiltonian

$$H = U^\dagger \tilde{\mathcal{H}} U = \frac{\omega_0}{2}\sigma_{z0} + \frac{\varepsilon}{2}\sigma_{z1} - \frac{\Delta}{2}\sigma_{x1} + H_B + \sum_k g_k(b_k + b_k^\dagger)\sigma_{z1} + \frac{a}{2}\sigma_{z0}\sigma_{z1} \tag{3}$$

After the application of the above polaron transformation, the chromophore−phonon coupling is removed from the Hamiltonian at the expense of introducing an explicit form of the chromophore−TLS coupling, which arises from an indirect, phonon-mediated interaction. This description allows for a convenient, perturbative treatment.[5] We shall take the dressed Hamiltonian (eq 3) as our starting point. Throughout this paper, the spectral density $J(\omega) = \Sigma_k |g_k|^2 \delta(\omega - \omega_k) = \kappa \omega_{ph}^{-2} \omega^l e^{(-\omega/\omega_c)}$ is assumed with l being the spectral exponent. The cutoff frequency is $\omega_c = 4$, and ω_{ph} is the characteristic phonon frequency that will be used as the energy unit. κ is a dimensionless constant representing the TLS−phonon coupling strength. We adopt $l = 3$ (super-Ohmic form) in all the calculations. The parameter $a = (\gamma\eta)/(2r^3)$ has the radial and angular dependence of a dipole−dipole interaction, where γ is the TLS−chromophore coupling constant, and r is the distance between them. The orientation parameter, η, which in principle could assume a continuum of values corresponding to rotations of the TLS in space, is set to $\eta = \pm 1$ for simplicity. In the following calculations, we simply consider a as the coupling parameter between the TLS and the chromophore.[5]

It is easy to see that the operator σ_{z0} is a conservative quantity. The definition of the pseudospin operators can be written as

$$\sigma_{z0} = |e\rangle\langle e| - |g\rangle\langle g| \qquad \sigma_{x0} = |g\rangle\langle e| + |e\rangle\langle g| \tag{4}$$

where g (e) is the ground (excited) state of the chromophore, and

$$\sigma_{z1} = |\uparrow\rangle\langle\uparrow| - |\downarrow\rangle\langle\downarrow| \qquad \sigma_{x1} = |\uparrow\rangle\langle\downarrow| + |\downarrow\rangle\langle\uparrow| \tag{5}$$

where $\uparrow$ ($\downarrow$) is the upper (lower) state of the TLS. Next, we will adopt the recently proposed TCL polaron master equation approach.[8,25,41] The polaron transformation is generated by $S = \Sigma_k (g_k/\omega_k)(b_k^\dagger - b_k)(\sigma_{z1})/2$, resulting in the transformed Hamiltonian

$$\tilde{H} = e^S H e^{-S} = \tilde{H}_0 + \tilde{H}_1 + H_B \tag{6}$$

$$\tilde{H}_0 = \frac{\omega_0}{2}\sigma_{z0} + \frac{\varepsilon}{2}\sigma_{z1} - \frac{\Delta}{2}\sigma_{x1}\Theta - \sum_k \frac{g_k^2}{4\omega_k} + \frac{a}{2}\sigma_{z0}\sigma_{z1} \tag{7}$$

$$\tilde{H}_1 = -\frac{\Delta}{2}[\sigma_{x1}(\cosh B - \Theta) + i\sigma_{y1}\sinh B] \tag{8}$$

where $B = \sum_k (g_k/\omega_k)(b_k^\dagger - b_k)$ and $\Theta = \langle \cosh B\rangle = \exp[-(1/2)\sum_k (g_k/\omega_k)^2 \coth(\beta\omega_k/2)]$. Here, we assume that the phonon bath is in thermal equilibrium at temperature $T = (k_B\beta)^{-1}$ with Boltzmann constant k_B. The TCL equation up to the second order in the interaction picture is known as[8,25,47]

$$\frac{\partial \mathcal{P}\tilde{\rho}_I(t)}{\partial t} = \mathcal{P}\tilde{\mathcal{L}}(t)\mathcal{Q}\tilde{\rho}_I(0) + \int_0^t ds \mathcal{P}\tilde{\mathcal{L}}(t)\tilde{\mathcal{L}}(s)\mathcal{Q}\tilde{\rho}_I(0) + \int_0^t ds \mathcal{P}\tilde{\mathcal{L}}(t)\tilde{\mathcal{L}}(s)\mathcal{P}\tilde{\rho}_I(t) \tag{9}$$

The first two terms in the right-hand side (r.h.s.) of eq 9 are inhomogeneous terms. They are nonzero only when the initial bath state differs from the reference state ρ_B chosen to be the thermal equilibrium state. In our case, we shall see that this corresponds to a nonequilibrium preparation of the initial environmental state within the polaron frame. $\tilde{\rho}_I(t)$ is the entire density matrix in the polaron frame. The superoperator $\mathcal{P}$ is defined by $\mathcal{P}(\cdot) = \mathrm{Tr}_B(\cdot)\otimes\rho_B$ and $\mathcal{Q} = 1 - \mathcal{P}$. Furthermore, the superoperator $\tilde{\mathcal{L}}$ is defined by $\tilde{\mathcal{L}}(t)(\cdot) = -i[\tilde{H}_{1I}(t), \cdot]$. $\tilde{H}_{1I}(t)$ is given by

$$\tilde{H}_{1I}(t) = e^{i(\tilde{H}_0 + H_B)t}\tilde{H}_1 e^{-i(\tilde{H}_0 + H_B)t} = -\frac{\Delta}{2}[\sigma_{+1}(t)D(t) + \sigma_{-1}(t)D^\dagger(t)] \qquad D(t) = e^{B(t)} - \Theta \tag{10}$$

where $\sigma_{\pm 1}(t) = e^{i\tilde{H}_0 t}\sigma_{\pm 1} e^{-i\tilde{H}_0 t}$ and $B(t) = \Sigma_k (g_k)/(\omega_k)(b_k^\dagger e^{i\omega_k t} - b_k e^{-i\omega_k t})$. σ_{+1} (σ_{-1}) is an effective raising (lowering) operator of the TLS. It is convenient to express them in the eigen-state space in the interaction picture. First, we diagonalize the Hamiltonian in eq 7. The four energy levels and the corresponding eigenvectors are expressed as

dx.doi.org/10.1021/jp5000717 | J. Phys. Chem. A 2014, 118, 2220−2227

$$E_g^{\pm} = -\frac{\omega_0}{2} - \lambda \pm \sqrt{\left(\frac{\varepsilon - a}{2}\right)^2 + \left(\frac{\Delta\Theta}{2}\right)^2}$$

$$E_e^{\pm} = \frac{\omega_0}{2} - \lambda \pm \sqrt{\left(\frac{\varepsilon + a}{2}\right)^2 + \left(\frac{\Delta\Theta}{2}\right)^2}$$

$$|\psi_{g(e)}^{+}\rangle = \left(\cos\frac{\theta_{g(e)}}{2}|\uparrow\rangle + \sin\frac{\theta_{g(e)}}{2}|\downarrow\rangle\right) \otimes |g(e)\rangle$$

$$|\psi_{g(e)}^{-}\rangle = \left(-\sin\frac{\theta_{g(e)}}{2}|\uparrow\rangle + \cos\frac{\theta_{g(e)}}{2}|\downarrow\rangle\right) \otimes |g(e)\rangle \tag{11}$$

where $\lambda = \Sigma_k(g_k^2)/(4\omega_k)$, and $\tan\theta_g = (-\Delta\Theta)/(\varepsilon - a)$ ($\tan\theta_e = (-\Delta\Theta)/(\varepsilon + a)$). According to eq 11, in the eigen-state representation we can easily obtain the expressions of the operators in the interaction picture. Let $\rho_{s(I)}(t)$ and $\sigma_{s(I)}(t)$ denote the Schrödinger (interaction) picture density operators of the entire system and the sum of the chromophore and the TLS, respectively, while their counterparts in the polaron frame are labeled as $\tilde{\rho}_{s(I)}(t)$ and $\tilde{\sigma}_{s(I)}(t)$. In the Schrödinger picture and the polaron frame, quantum master equation (QME) is given by

$$\begin{aligned}\dot{\tilde{\sigma}}_s(t) = &-i[\tilde{H}_0, \tilde{\sigma}_s(t)] - i\mathrm{Tr}_B\{e^{-i\tilde{H}_0't}[\tilde{H}_{1I}(t), Q\tilde{\rho}_I(0)]e^{i\tilde{H}_0't}\} \\ &- \int_0^t ds\mathrm{Tr}_B\{e^{-i\tilde{H}_0't}[\tilde{H}_{1I}(t), [\tilde{H}_{1I}(s), Q\tilde{\rho}_I(0)]]e^{i\tilde{H}_0't}\} \\ &- \int_0^t ds\mathrm{Tr}_B\{[\tilde{H}_{1I}(0), [\tilde{H}_{1I}(s-t), \tilde{\sigma}_s(t) \otimes \rho_B]]\}\end{aligned} \tag{12}$$

where $\tilde{H}_0' = \tilde{H}_0 + H_B$. The factorized initial state $\rho(0)$ is assumed in the calculation of the dynamics

$$\begin{aligned}\rho(0) &= \begin{pmatrix} \frac{1}{2} & \frac{1}{2} \\ \frac{1}{2} & \frac{1}{2} \end{pmatrix}^C \otimes |\uparrow\rangle\langle\uparrow|^{TLS} \otimes \rho_B \\ &= \sigma(0) \otimes \rho_B\end{aligned} \tag{13}$$

where $\rho_B = e^{-\beta H_B}/Z_B$ and the boson bath is in thermal equilibrium with partition functions given by Z_B. The density operators of the chromophore and the TLS are prepared initially in a pure state. In the polaron frame, we obtain $\tilde{\rho}(0) = \sigma(0) \otimes \tilde{\rho}_B$, where $\tilde{\rho}_B = e^{1/2B}\rho_B e^{-1/2B}$. Further, one has $Q\tilde{\rho}_I(0) = \tilde{\rho}(0) - \mathrm{Tr}_B\{\tilde{\rho}(0)\} \otimes \rho_B = \sigma(0) \otimes (\tilde{\rho}_B - \rho_B)$. The derivation of the explicit forms of the QME and the two-time correlation functions is shown in Appendix A.

III. NON-MARKOVIAN DYNAMICS IN THE LAB FRAME

Generally, the expectation value of the system (chromophore+TLS) observable A in the lab frame is given by[8,25,41]

$$\begin{aligned}\langle A\rangle &= \mathrm{Tr}_{S+B}\{A\rho_s(t)\} \\ &= \mathrm{Tr}_{S+B}\{e^S A\, e^{-S}\mathcal{P}\tilde{\rho}_s(t)\} + \mathrm{Tr}_{S+B}\{e^S A\, e^{-S}Q\tilde{\rho}_s(t)\} \\ &= \langle A\rangle_{rel} + \langle A\rangle_{irrel}\end{aligned} \tag{14}$$

where $\langle A\rangle_{rel} = \mathrm{Tr}_S\{\tilde{A}\tilde{\sigma}_s(t)\}$ and $\tilde{A} = \mathrm{Tr}_B\{e^S A\, e^{-S}\rho_B\}$. $\langle A\rangle_{irrel} = \mathrm{Tr}_{S+B}\{e^S A\, e^{-S}\, e^{-i\tilde{H}_0't}Q\tilde{\rho}_I(t)\, e^{i\tilde{H}_0't}\}$. To the zeroth order the irrelevant contribution becomes $\langle A\rangle_{irrel} \simeq \mathrm{Tr}_{S+B}\{e^{i\tilde{H}_0't}e^S A\, e^{-S}\, e^{-i\tilde{H}_0't}Q\tilde{\rho}_I(0)\}$. This approximation is applied to evaluate the irrelevant expectation values in the calculation of the dynamical properties. Note that the irrelevant part of the expectation value vanishes if $[A, S] = 0$. The dynamics of the chromophore and the TLS can be obtained based on eqs 13 and 14, such as

$$\begin{aligned}\langle\sigma_{x(y)0}\rangle_{rel} &= \mathrm{Tr}_S\{\tilde{\sigma}_s(t)\sigma_{x(y)0}\} \\ \langle\sigma_{z1}\rangle_{rel} &= \mathrm{Tr}_S\{\tilde{\sigma}_s(t)\sigma_{z1}\} \\ \langle\sigma_{x(y)1}\rangle_{rel} &= \Theta\mathrm{Tr}_S\{\tilde{\sigma}_s(t)\sigma_{x(y)1}\} \\ \langle\sigma_{x(y)0}\rangle_{irrel} &= 0 \\ \langle\sigma_{z1}\rangle_{irrel} &= 0 \\ \langle\sigma_{x1}\rangle_{irrel} &= \Theta\mathrm{Tr}_S\{\sigma(0)\sigma_{+1}(t)\}d(t) + c.c. \\ \langle\sigma_{y1}\rangle_{irrel} &= -i\Theta\mathrm{Tr}_S\{\sigma(0)\sigma_{+1}(t)\}d(t) + c.c.\end{aligned} \tag{15}$$

where $d(t) = \exp[i\sum_k (g_k^2/\omega_k^2)\sin(\omega_k t)] - 1$.

Furthermore, in order to quantify the entanglement between the system (i.e., the chromophore and the TLS) and the bath, we evaluate the evolution of the von Neumann entropy. If $\sigma_s(t)$ is the reduced density matrix of the system in the original basis, the von Neumann entropy of the system, which changes with time due to dephasing and relaxation processes induced by the bath, is given by[46−51]

$$\mathcal{S}(\sigma_s(t)) = \mathrm{Tr}(\sigma_s(t)\ln\sigma_s(t)) \tag{16}$$

In addition, we can also calculate the linear absorption lineshape function[5]

$$I(\omega) = \frac{1}{\pi}\mathrm{Re}\int_0^\infty e^{i\omega t}\langle\mu(t)\mu(0)\rangle\, dt \tag{17}$$

where $\mu(0) = \sigma_{x0}$ is the initial dipole moment operator in the Condon approximation, and $\mu(t) = e^{iHt}\mu(0)e^{-iHt}$ is the same operator at time t in the Heisenberg picture. The dipole autocorrelation function in the polaron frame is given by

$$\langle\mu(t)\mu(0)\rangle = \mathrm{Tr}_{S+B}\{\tilde{\rho}_1(0)\, e^{i\tilde{H}t}\sigma_{x0}\, e^{-i\tilde{H}t}\sigma_{x0}\} \tag{18}$$

Note that the average value of the irrelevant part in eq 18 is zero. In the calculation of the linear absorption spectrum, we have assumed $\varepsilon \gg a$, $\varepsilon \gg \Delta$, and $\omega_0 \gg a$ so that the equilibrium density matrix for the chromophore (the TLS) is given by[3]

$$\rho_{C(TLS)}^{eq} \simeq P_{e(\uparrow)}|e(\uparrow)\rangle\langle e(\uparrow)| + P_{g(\downarrow)}|g(\downarrow)\rangle\langle g(\downarrow)| \tag{19}$$

where $P_e = [2e^{\beta\omega_0/2}\cosh(\beta\omega_0/2)]^{-1}$, $P_g = [2e^{-\beta\omega_0/2}\cosh(\beta\omega_0/2)]^{-1}$, $P_\uparrow = [2e^{\beta\epsilon/2}\cosh(\beta\epsilon/2)]^{-1}$, and $P_\downarrow = [2e^{-\beta\epsilon/2}\cosh(\beta\epsilon/2)]^{-1}$. The parameter regime of interest here corresponds to a low-temperature realistic glassy system. In the lab frame, the factorized initial condition for the total system is assumed to be

$$\rho_1(0) = \rho_C^{eq} \otimes \rho_{TLS}^{eq} \otimes \rho_B \tag{20}$$

Furthermore, in the polaron frame, one has the initial density matrix

dx.doi.org/10.1021/jp5000717 | J. Phys. Chem. A 2014, 118, 2220−2227

$$\tilde{\rho}_I(0) = \rho_C^{eq} \otimes (P_\uparrow |\uparrow\rangle\langle\uparrow| \otimes e^{1/2B}\rho_B e^{-1/2B} + P_\downarrow |\downarrow\rangle\langle\downarrow| \otimes e^{-1/2B}\rho_B e^{1/2B}) \quad (21)$$

IV. RESULTS AND DISCUSSION

The typical parameter set derived experimentally for terrylene in polystyrene[5] consists of ε_{max} = 17 K, $\Delta = 2.8 \times 10^{-7}$ K to 17 K, a_{max} = 4.5 K, and T = 0.1 to 10 K. In all the calculations, we set ω_{ph} = 2 K as the energy unit.

We now examine the dissipative dynamics of the chromophore and the TLS based on eqs 15 and 16, as shown in Figure 1.

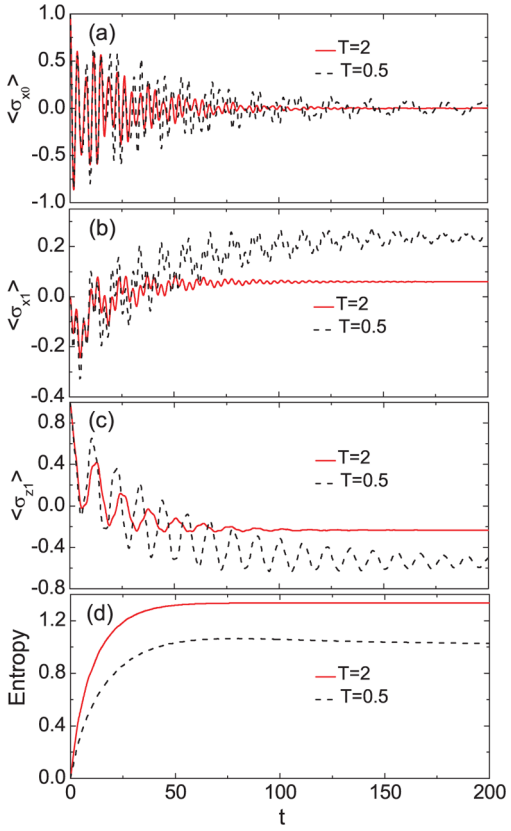

Figure 1. Dynamics of the chromophore and the TLS for two bath temperatures, T = 0.5 and T = 2.0. Other parameters are ω_0 = 1, ε = 1, Δ = 0.8, a = 0.8, κ = 0.05. (a) Evolution of the coherence of the chromophore. (b) Evolution of the coherence of the TLS. (c) Evolution of the population difference of the TLS. (d) Evolution of the von Neumann entropy of the chromophore−TLS system.

The operator σ_{z0} commutes with the Hamiltonian 3, and $\langle\sigma_{z0}\rangle$ is a constant of motion, i.e., the population of the chromophore does not change with the time. However, the pure dephasing mechanism still exists because the chromophore is indirectly coupled with the bath, as shown in Figure 1a. The decoherence process is faster at a higher temperature and $\langle\sigma_{x0}\rangle$ reaches the steady state value 0. The evolution of the coherence of the TLS is plotted in Figure 1b. The population relaxation and the pure dephasing processes occur in the TLS. At long times the coherence of the TLS reaches a plateau, the height of which decreases with an increase in the temperature.

The population difference of the TLS, $\langle\sigma_{z1}\rangle$, is also investigated, and the results are shown in Figure 1c. The steady state value of the population difference demonstrates that the TLS is thermally equilibrated. In the high-temperature limit, for example, $\langle\sigma_{z1}\rangle$ approaches zero due to equal occupation of the two levels. In general, it is found that $\langle\sigma_{z1}\rangle$ undergoes damped oscillations, and the oscillation frequency is reduced as the temperature is increased.

In addition, plotted in Figure 1d is the von Neumann entropy of the entire system of the chromophore and the TLS. The linearized form of the von Neumann entropy has been previously used to quantify exciton−phonon entanglement in the Holstein Hamiltonian.[46,52] As is well-known, the von Neumann entropy is bounded from above $\mathcal{S}(\sigma_s(t)) \leq \ln \mathcal{D}$, where $\mathcal{D}$ is the dimension of the Hilbert space of the system. Therefore, the entropy may be bigger than 1 in our case. $\mathcal{S}(\sigma_s(t))$ is equal to zero due to the factorized initial condition, and increases with the time evolution. At about t = 50, it reaches a plateau. Higher temperature gives rise to a higher plateau. In the limit of infinite temperature, $\mathcal{S}(\sigma_s(t))$ achieves the largest value possible, ln 4, that is, arriving at the completely mixed state.

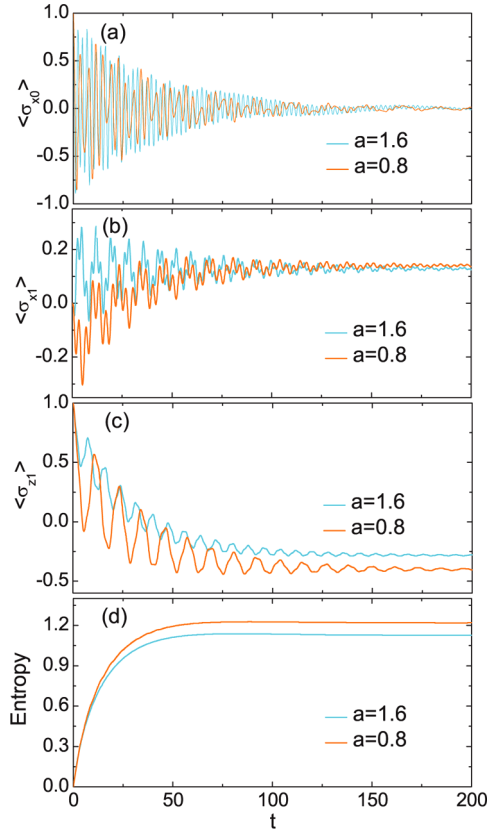

Figure 2. Dynamics of the chromophore and the TLS for two coupling strengths, a = 0.8 and a = 1.6. Other parameters are ω_0 = 1, ε = 1, Δ = 0.8, T = 1, κ = 0.05. (a) Evolution of the coherence of the chromophore. (b) Evolution of the coherence of the TLS. (c) Evolution of the population difference of the TLS. (d) Evolution of the von Neumann entropy of the chromophore−TLS system.

The effect of the coupling between the chromophore and the TLS on the dynamics is also interesting, as shown in Figure 2. For the chromophore, the oscillation frequency of the coherence increases with increasing coupling parameter a. From Figure 2a, it is observed that the dephasing time is not evidently connected with the coupling strength between the chromophore and the TLS. Initially, the evolution of the TLS coherence is sensitive to the coupling strength a, and a larger a brings about a larger $\langle\sigma_{x1}\rangle$,

dx.doi.org/10.1021/jp5000717 | J. Phys. Chem. A 2014, 118, 2220−2227

while in the steady state, the impact of a on the coherence is minimal, as shown in Figure 2b. In addition, it is found in Figure 2c that the steady-state population difference of the TLS, $\langle\sigma_{z1}\rangle$, increases with an increase in the coupling parameter a. In the limit of $a \to \infty$, from eq 11 the energy levels approach $E^{\pm}_{g(e)} = \pm\infty$ with only the ground states $E^{-}_{g(e)}$ occupied, and one also has $\theta_g \to 0$ and $\theta_e \to 2\pi$, which can be substituted into the wave functions of eq 11. It is then found that the wave functions of the two degenerate ground states satisfy the asymptotical relations $|\psi_{g(e)}^{-}\rangle \to |\downarrow\rangle(|\uparrow\rangle)\otimes|g(e)\rangle$, and the two states in the TLS ($|\downarrow\rangle$ and $|\uparrow\rangle$) are equally occupied, i.e., $\langle\sigma_{z1}(\infty)\rangle \to 0$ in the limit of $a \to \infty$. On the other hand, the von Neumann entropy of the system has a bigger saturation value for weaker coupling between the chromophore and the TLS, as shown in Figure 2d. It is interesting that the temperature effect on the entanglement entropy is found to be opposite to that of the coupling parameter a upon comparing Figure 1d with Figure 2d.

To facilitate the investigation of the linear absorption spectrum of the TLS−chromophore system, a finite radiative lifetime for the chromophore, $\gamma_{\rm rad}$, is introduced in our computation to ensure that there is a finite width for spectral peaks. The effect of temperature on the spectra is demonstrated in Figure 3 for two chromophore−TLS coupling strengths, a = 0.1, 0.2. Other parameters adopted are $\omega_0 = 1$, $\varepsilon = 2$, $\kappa = 0.05$, $\Delta = 0.1$, and $\gamma_{\rm rad} = 0.03$. Two transitions $E^{\pm}_g \to E^{\pm}_e$ occur in our case. The oscillator strength of $E^{-}_g \to E^{-}_e$ is greater at lower temperatures. Note that the factorized initial condition is assumed. The oscillator strength is proportional to the occupation probability of the energy level $E^{\pm}_g$. Therefore, we can expect that the transition strength of $E^{+}_g \to E^{+}_e$ will increase with the increase of the temperature, as shown in Figure 3a,b. From eq 11, the coupling strength a determines the splitting of the energy levels, and as a result, the two absorption peaks move away from each other with an increase in a, as shown in Figure 3b.

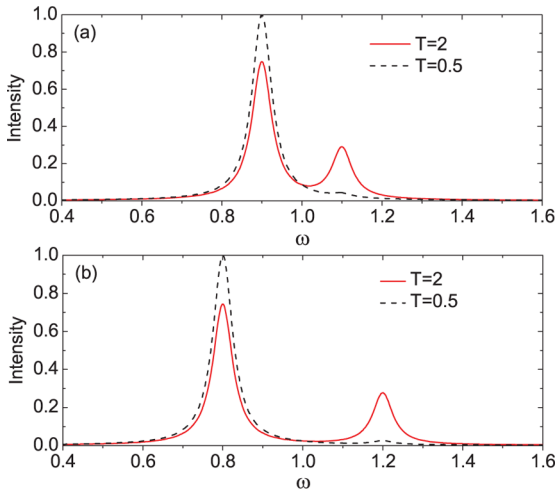

Figure 3. Linear absorption spectra for two temperatures, T = 2 (solid line) and T = 0.5 (dashed line). Two strengths of TLS−chromophore coupling are used: (a) a = 0.1; (b) a = 0.2.

Only one TLS has been considered in our discussion here. However, it is also interesting to look into the effect of multiple TLSs on the line shape of the absorption spectrum. In fact, it has been shown that strong chromophore−TLS coupling due to their close proximity results in non-Gaussian features in absorption spectra.[53,54] In a realistic system, TLS−TLS interactions induced by strain fields can also exist, and their effect was investigated by Brown et al.[5] who concluded that the TLS−TLS coupling does not exert any significantly direct effect on the chromophore's spectral properties, including the line width histograms, and that only in relatively rare cases does this coupling affect the single molecule line shapes. Further discussion of the TLS−TLS interactions and their effect on the absorption line shape, however, is beyond the scope of this work. Due to the equivalence between the quantum microscopic model (eq 3) and the stochastic sudden-jump treatments,[3] some discussion on its implications to the line shape is in order. Firstly, we assume the individual contributions from each TLS to the line shape are small, thereby giving rise to the observed central limit type behavior of the line shape as the cumulative effect of many small perturbations. Within the stochastic sudden-jump treatment, the transition frequency of the chromophore depends upon the instantaneous states of the TLS, and each flipping TLS modifies the chromophore transition frequency. As the two absorption peaks move away from each other with an increase in the chromophore−TLS coupling, the line shape can morph from Gaussian to Lorentzian. Accordingly, we have shown that line shape computed in our model closely resembles that from the uncoupled sudden-jump model.[5] The observed shapes of single molecule lines are primarily the result of splitting of the chromophore's absorption peak into many overlapping lifetime limited Lorentzians. The relative heights of these Lorentzians are dominated by the occupation probabilities of the energy level $E^{\pm}_g$, and the splittings themselves are dependent upon the chromophore−TLS separations. In addition, for the multi-TLS environment, the resultant line shape is Gaussian in the absence of disorder but becomes Lorentzian for completely disordered TLSs in the long time limit.[54] Due to the low TLS density in glass, the TLS−TLS coupling will have insignificant influence on the line width histograms.[5]

V. CONCLUSION

In summary, we have employed the time-convolutionless polaron master equation method to investigate the dissipative dynamics of a central chromophore embedded in a bath of two-level systems commonly found in low-temperature glasses. Our theory includes inhomogeneous terms which account for nonequilibrium initial preparation effects, and it goes beyond the weak resonance coupling limit of the Förster and Dexter theory.[55,56] By treating the relevant degrees of freedom in a polaron frame, this theory is valid for moderate spin-phonon coupling and is capable of handling initial nonequilibrium bath states and spatially correlated environments. The other advantage is the higher computational efficiency of our dynamics calculations as compared to other nonperturbative approaches. It is found that the TLS population difference undergoes damped oscillation, and its oscillation frequency is reduced as the temperature is increased, while the oscillation frequency of the chromophore coherence increases with an increase in the coupling parameter a. The temperature effect on the entanglement entropy goes counter to that of the coupling parameter a. In addition, the oscillator strength in the linear absorption spectra is found to be modified by the temperature. As the two peaks in the absorption spectrum move away from each other with an increasing chromophore−TLS coupling strength, strong coupling adds non-Gaussian deviations to the absorption line shape in a multi-TLS environment.

dx.doi.org/10.1021/jp5000717 | J. Phys. Chem. A 2014, 118, 2220−2227

APPENDIX A: THE QME AND THE TWO-TIME CORRELATION FUNCTIONS

The second term of the r.h.s. in eq 12 can be written as

$$
\begin{aligned}
&-i\mathrm{Tr}_B\{e^{-i\tilde{H}_0't}[\tilde{H}_{1I}(t), Q\tilde{\rho}_I(0)]e^{i\tilde{H}_0't}\}\\
&= i\left[\frac{\Delta}{2}\sigma_{+1}e^{-i\tilde{H}_0t}\sigma(0)e^{i\tilde{H}_0t}\right]\mathrm{Tr}_B\{D(e^{-iH_Bt}\tilde{\rho}_Be^{iH_Bt}-\rho_B)\}\\
&\quad + i\left[\frac{\Delta}{2}\sigma_{-1}e^{-i\tilde{H}_0t}\sigma(0)e^{i\tilde{H}_0t}\right]\mathrm{Tr}_B\{D^\dagger(e^{-iH_Bt}\tilde{\rho}_Be^{iH_Bt}-\rho_B)\}\\
&\quad - i\left[\frac{\Delta}{2}e^{-i\tilde{H}_0t}\sigma(0)e^{i\tilde{H}_0t}\sigma_{+1}\right]\mathrm{Tr}_B\{(e^{-iH_Bt}\tilde{\rho}_Be^{iH_Bt}-\rho_B)D\}\\
&\quad - i\left[\frac{\Delta}{2}e^{-i\tilde{H}_0t}\sigma(0)e^{i\tilde{H}_0t}\sigma_{-1}\right]\mathrm{Tr}_B\{(e^{-iH_Bt}\tilde{\rho}_Be^{iH_Bt}-\rho_B)D^\dagger\}
\end{aligned}
\tag{A1}
$$

where

$$
\begin{aligned}
\mathrm{Tr}_B\{D(e^{-iH_Bt}\tilde{\rho}_Be^{iH_Bt}-\rho_B)\} &= \Theta(e^{i\sum_k\frac{g_k^2}{\omega_k^2}\sin(\omega_kt)}-1)\\
&= \Theta\mathrm{d}(t)\\
\mathrm{Tr}_B\{(e^{-iH_Bt}\tilde{\rho}_Be^{iH_Bt}-\rho_B)D^\dagger\} &= \Theta\mathrm{d}(-t)
\end{aligned}
\tag{A2}
$$

The third term of the r.h.s. in eq 12 can be written as

$$
\begin{aligned}
&-\int_0^t \mathrm{d}s\mathrm{Tr}_B\{e^{-i\tilde{H}_0't}[\tilde{H}_{1I}(t),[\tilde{H}_{1I}(s),Q\tilde{\rho}_I(0)]]e^{i\tilde{H}_0't}\}\\
&= \left\{-\int_0^t \mathrm{d}s\left[\frac{\Delta^2}{4}\sigma_{+1}\sigma_{+1}(s-t)e^{-i\tilde{H}_0t}\sigma(0)e^{i\tilde{H}_0t}\right]\right.\\
&\qquad \mathrm{Tr}_B\{DD(s-t)(e^{-iH_Bt}\tilde{\rho}_Be^{iH_Bt}-\rho_B)\}\\
&\quad -\int_0^t \mathrm{d}s\left[\frac{\Delta^2}{4}\sigma_{+1}\sigma_{-1}(s-t)e^{-i\tilde{H}_0t}\sigma(0)e^{i\tilde{H}_0t}\right]\\
&\qquad \mathrm{Tr}_B\{DD^\dagger(s-t)(e^{-iH_Bt}\tilde{\rho}_Be^{iH_Bt}-\rho_B)\}\\
&\quad -\int_0^t \mathrm{d}s\left[\frac{\Delta^2}{4}\sigma_{-1}\sigma_{+1}(s-t)e^{-i\tilde{H}_0t}\sigma(0)e^{i\tilde{H}_0t}\right]\\
&\qquad \mathrm{Tr}_B\{D^\dagger D(s-t)(e^{-iH_Bt}\tilde{\rho}_Be^{iH_Bt}-\rho_B)\}\\
&\quad -\int_0^t \mathrm{d}s\left[\frac{\Delta^2}{4}\sigma_{-1}\sigma_{-1}(s-t)e^{-i\tilde{H}_0t}\sigma(0)e^{i\tilde{H}_0t}\right]\\
&\qquad \mathrm{Tr}_B\{D^\dagger D^\dagger(s-t)(e^{-iH_Bt}\tilde{\rho}_Be^{iH_Bt}-\rho_B)\}\\
&\quad +\int_0^t \mathrm{d}s\left[\frac{\Delta^2}{4}\sigma_{+1}(s-t)e^{-i\tilde{H}_0t}\sigma(0)e^{i\tilde{H}_0t}\sigma_{+1}\right]\\
&\qquad \mathrm{Tr}_B\{D(s-t)(e^{-iH_Bt}\tilde{\rho}_Be^{iH_Bt}-\rho_B)D\}\\
&\quad +\int_0^t \mathrm{d}s\left[\frac{\Delta^2}{4}\sigma_{+1}(s-t)e^{-i\tilde{H}_0t}\sigma(0)e^{i\tilde{H}_0t}\sigma_{-1}\right]\\
&\qquad \mathrm{Tr}_B\{D(s-t)(e^{-iH_Bt}\tilde{\rho}_Be^{iH_Bt}-\rho_B)D^\dagger\}\\
&\quad +\int_0^t \mathrm{d}s\left[\frac{\Delta^2}{4}\sigma_{-1}(s-t)e^{-i\tilde{H}_0t}\sigma(0)e^{i\tilde{H}_0t}\sigma_{+1}\right]\\
&\qquad \mathrm{Tr}_B\{D^\dagger(s-t)(e^{-iH_Bt}\tilde{\rho}_Be^{iH_Bt}-\rho_B)D\}\\
&\quad \left.+\int_0^t \mathrm{d}s\left[\frac{\Delta^2}{4}\sigma_{-1}(s-t)e^{-i\tilde{H}_0t}\sigma(0)e^{i\tilde{H}_0t}\sigma_{-1}\right]\right.\\
&\qquad \left.\mathrm{Tr}_B\{D^\dagger(s-t)(e^{-iH_Bt}\tilde{\rho}_Be^{iH_Bt}-\rho_B)D^\dagger\}\right\}\\
&\qquad +h.\ c.
\end{aligned}
\tag{A3}
$$

where

$$
\begin{aligned}
&\mathrm{Tr}_B\{DD(s-t)(e^{-iH_Bt}\tilde{\rho}_Be^{iH_Bt}-\rho_B)\}\\
&= \mathrm{Tr}_B\{\tilde{\rho}_B(e^{B(t)}-\Theta)(e^{B(s)}-\Theta)\}-\mathrm{Tr}_B\{\rho_BD(t)D(s)\}\\
&= \mathrm{Tr}_B\{\tilde{\rho}_Be^{B(t)+B(s)}\}e^{1/2[B(t),B(s)]}-\Theta^2[d(t)+d(s)+1]\\
&\quad -\mathrm{Tr}_B\{\rho_BD(t)D(s)\}\\
&= e^{-\phi(0)}\{e^{-\phi(t-s)}d(t)d(s)+(e^{-\phi(t-s)}-1)[d(t)+d(s)]\}\\
&\qquad \mathrm{Tr}_B\{DD^\dagger(s-t)(e^{-iH_Bt}\tilde{\rho}_Be^{iH_Bt}-\rho_B)\}\\
&= e^{-\phi(0)}\{e^{\phi(t-s)}d(t)d^*(s)+(e^{\phi(t-s)}-1)[d(t)+d^*(s)]\}\\
&\qquad \mathrm{Tr}_B\{D^\dagger D(s-t)(e^{-iH_Bt}\tilde{\rho}_Be^{iH_Bt}-\rho_B)\}\\
&= e^{-\phi(0)}\{e^{\phi(t-s)}d^*(t)d(s)+(e^{\phi(t-s)}-1)[d^*(t)+d(s)]\}\\
&\qquad \mathrm{Tr}_B\{D^\dagger D^\dagger(s-t)(e^{-iH_Bt}\tilde{\rho}_Be^{iH_Bt}-\rho_B)\}\\
&= e^{-\phi(0)}\{e^{-\phi(t-s)}d^*(t)d^*(s)+(e^{-\phi(t-s)}-1)\\
&\qquad [d^*(t)+d^*(s)]\}
\end{aligned}
\tag{A4}
$$

In the calculation of eq A4, we have used the following two-time correlation functions

$$
\begin{aligned}
\mathrm{Tr}_B\{\rho_BD(t_1)D(t_2)\} &= e^{-\phi(0)}[e^{-\phi(t_1-t_2)}-1]\\
\mathrm{Tr}_B\{\rho_BD(t_1)D^\dagger(t_2)\} &= e^{-\phi(0)}[e^{\phi(t_1-t_2)}-1]\\
\mathrm{Tr}_B\{\rho_BD^\dagger(t_1)D(t_2)\} &= \mathrm{Tr}_B\{\rho_BD(t_1)D^\dagger(t_2)\}\\
\mathrm{Tr}_B\{\rho_BD^\dagger(t_1)D^\dagger(t_2)\} &= \mathrm{Tr}_B\{\rho_BD(t_1)D(t_2)\}
\end{aligned}
\tag{A5}
$$

where $\phi(t)=\Sigma_k(g_k/\omega_k)^2(\cos\omega_kt\coth(\beta\omega_k/2)-i\sin\omega_kt)$. The last term of the r.h.s. in eq 12 can be written as

$$
\begin{aligned}
&-\int_0^t \mathrm{d}s\mathrm{Tr}_B\{[\tilde{H}_{1I}(0),[\tilde{H}_{1I}(s-t),\tilde{\sigma}_s(t)\otimes\rho_B]]\}\\
&= \left\{-\int_0^t \mathrm{d}s\left[\frac{\Delta^2}{4}\sigma_{+1}\sigma_{+1}(s-t)\tilde{\sigma}_s(t)\right]\mathrm{Tr}_B\{\rho_BDD(s-t)\}\right.\\
&\quad -\int_0^t \mathrm{d}s\left[\frac{\Delta^2}{4}\sigma_{+1}\sigma_{-1}(s-t)\tilde{\sigma}_s(t)\right]\mathrm{Tr}_B\{\rho_BDD^\dagger(s-t)\}\\
&\quad -\int_0^t \mathrm{d}s\left[\frac{\Delta^2}{4}\sigma_{-1}\sigma_{+1}(s-t)\tilde{\sigma}_s(t)\right]\mathrm{Tr}_B\{\rho_BD^\dagger D(s-t)\}\\
&\quad -\int_0^t \mathrm{d}s\left[\frac{\Delta^2}{4}\sigma_{-1}\sigma_{-1}(s-t)\tilde{\sigma}_s(t)\right]\mathrm{Tr}_B\{\rho_BD^\dagger D^\dagger(s-t)\}\\
&\quad +\int_0^t \mathrm{d}s\left[\frac{\Delta^2}{4}\sigma_{+1}(s-t)\tilde{\sigma}_s(t)\sigma_{+1}\right]\mathrm{Tr}_B\{D(s-t)\rho_BD\}\\
&\quad +\int_0^t \mathrm{d}s\left[\frac{\Delta^2}{4}\sigma_{+1}(s-t)\tilde{\sigma}_s(t)\sigma_{-1}\right]\mathrm{Tr}_B\{D(s-t)\rho_BD^\dagger\}\\
&\quad +\int_0^t \mathrm{d}s\left[\frac{\Delta^2}{4}\sigma_{-1}(s-t)\tilde{\sigma}_s(t)\sigma_{+1}\right]\mathrm{Tr}_B\{D^\dagger(s-t)\rho_BD\}\\
&\quad \left.+\int_0^t \mathrm{d}s\left[\frac{\Delta^2}{4}\sigma_{-1}(s-t)\tilde{\sigma}_s(t)\sigma_{-1}\right]\mathrm{Tr}_B\{D^\dagger(s-t)\rho_BD^\dagger\}\right\}\\
&\qquad +h.\ c..
\end{aligned}
\tag{A6}
$$

Substituting the above eqs A1−A6 into eq 12, we can solve the motion equation of the reduced density matrix.

dx.doi.org/10.1021/jp5000717 | J. Phys. Chem. A 2014, 118, 2220−2227

AUTHOR INFORMATION

Corresponding Author

*E-mail: YZhao@ntu.edu.sg.

Notes

The authors declare no competing financial interest.

ACKNOWLEDGMENTS

Support from the Singapore National Research Foundation through the Competitive Research Programme (CRP) under Project No. NRF-CRP5-2009-04, the NNSF of China No. 11247238 (K.W.S.) and the Zhejiang Provincial Education Department Project No. Y201223209 (K.W.S.) are gratefully acknowledged.

REFERENCES

(1) Anderson, P. W.; Halperin, B. I.; Varma, C. M. Anomalous Low-Temperature Thermal Properties of Glasses and Spin Glasses. *Philos. Mag.* **1972**, *25*, 1−9.

(2) Phillips, W. A. Tunneling States in Amorphous Solids. *J. Low Temp. Phys.* **1972**, *7*, 351−360.

(3) Suárez, A.; Silbey, R. Study of a Microscopic Model for Two-Level System Dynamics in Glasses. *J. Phys. Chem.* **1994**, *98*, 7329−7336.

(4) Suárez, A.; Silbey, R. An Investigation of the Effects of Two Level System Coupling on Single Molecule Lineshapes in Low Temperature Glasses. *Chem. Phys. Lett.* **1994**, *218*, 445−453.

(5) Brown, F. L. H.; Silbey, R. J. An Investigation of the Effects of Two Level System Coupling on Single Molecule Lineshapes in Low Temperature Glasses. *J. Chem. Phys.* **1998**, *108*, 7434−7450.

(6) Heuer, A.; Silbey, R. J. Microscopic Description of Tunneling Systems in a Structural Model Glass. *Phys. Rev. Lett.* **1993**, *70*, 3911−3914.

(7) Dab, D.; Heuer, A.; Silbey, R. J. Low Temperature Properties of Glasses: A Preliminary Study of Double Well Potentials Microscopic Structure. *J. Lumin.* **1995**, *64*, 95−100.

(8) Wu, N.; Zhao, Y. Dynamics of a Two-Level System under the Simultaneous Influence of a Spin Bath and a Boson Bath. *J. Chem. Phys.* **2013**, *139*, 054118.

(9) Wang, C.; Zhang, Y. Y.; Chen, Q. H. Quantum Correlations in the Collective Spin Systems. *Phys. Rev. A* **2012**, *85*, 052112.

(10) Zhang, Y. Y.; Chen, Q. H.; Wang, K. L. Quantum Phase Transition in the Sub-Ohmic Spin-Boson Model: An Extended Coherent-State Approach. *Phys. Rev. B* **2010**, *81*, 121105.

(11) Fleury, L.; Zumbrusch, A.; Brown, R.; Bernard, J. Spectral Diffusion and Individual Two-level Systems Probed by Fluorescence of Single Terrylene Molecules in a Polyethylene Matrix. *J. Lumin.* **1993**, *56*, 15−28.

(12) Kozankiewicz, B.; Bernard, J.; Orrit, M. Single Molecule Lines and Spectral Hole Burning of Terrylene in Different Matrices. *J. Chem. Phys.* **1994**, *101*, 9377−9383.

(13) Kettner, R.; Tittel, J.; Basche, T.; Brauchle, C. Optical Spectroscopy and Spectral Diffusion of Single Dye Molecules in Amorphous Spin-Coated Polymer Films. *J. Phys. Chem.* **1994**, *98*, 6671−6674.

(14) Tillel, J.; Kettner, R.; Basche, T.; Brauchle, C.; Quante, H.; Mullen, K. Spectral Diffusion in an Amorphous Polymer Probed by Single Molecule Spectroscopy. *J. Lumin.* **1995**, *64*, 1−11.

(15) Reilly, P. D.; Skinner, J. L. Spectroscopy of a Chromophore Coupled to a Lattice of Dynamic Two-Level Systems: I. Absorption Lineshape. *J. Chem. Phys.* **1994**, *101*, 959−964; Spectral Diffusion of Single Molecule Fluorescence: A Probe of Low-Frequency Localized Excitations in Disordered Crystals. *Phys. Rev. Lett.* **1993**, *71*, 4257−4260.

(16) Bai, Y. S.; Fayer, M. D. Time Scales and Optical Dephasing Measurements: Investigation of Dynamics in Complex Systems. *Phys. Rev. B* **1989**, *39*, 11066−11084.

(17) Littau, K.-A.; Bai, Y. S.; Fayer, M. D. Two-Level Systems and Low-Temperature Glass Dynamics: Spectral Diffusion and Thermal Reversibility of Hole-Burning Linewidths. *J. Chem. Phys.* **1990**, *92*, 4145−4158.

(18) Meijers, H. C.; Wiersma, D. A. Glass Dynamics Probed by the Long-Lived Stimulated Photon Echo. *Phys. Rev. Lett.* **1992**, *68*, 381−384.

(19) Wannemacher, R.; Koedijk, J. M. A.; Volker, S. Spectral Diffusion in Organic Glasses-Temperature-Dependence of Permanent and Transient Holes. *Chem. Phys. Lett.* **1993**, *206*, 1−8.

(20) Sevian, H. M.; Skinner, J. L. Molecular Theory of Transition Energy Correlations for Pairs of Chromophores in Liquids or Glasses. *J. Chem. Phys.* **1992**, *97*, 8−18.

(21) Stoneham, A. M. Shapes of Inhomogeneously Broadened Resonance Lines in Solids. *Rev. Mod. Phys.* **1969**, *41*, 82−108.

(22) Messing, I.; Raz, B.; Jortner, J. Medium Perturbations of Atomic Extravalence Excitations. *J. Chem. Phys.* **1977**, *66*, 2239−2251.

(23) Jang, S. Theory of Multichromophoric Coherent Resonance Energy Transfer: A Polaronic Quantum Master Equation Approach. *J. Chem. Phys.* **2011**, *135*, 034105.

(24) Cheng, Y. C.; Fleming, G. R. Dynamics of Light Harvesting in Photosynthesis. *Annu. Rev. Phys. Chem.* **2009**, *60*, 241−262.

(25) Kolli, A.; Nazir, A.; Olaya-Castro, A. Electronic Excitation Dynamics in Multichromophoric Systems Described via a Polaron-Representation Master Equation. *J. Chem. Phys.* **2011**, *135*, 154112.

(26) Hughes, K. H.; Christ, C. D.; Burghardt, I. Effective-Mode Representation of Non-Markovian Dynamics: A Hierarchical Approximation of the Spectral Density. I. Application to Single Surface Dynamics. *J. Chem. Phys.* **2009**, *131*, 124108.

(27) Prior, J.; Chin, A. W.; Huelga, S. F.; Plenio, M. B. Efficient Simulation of Strong System-Environment Interactions. *Phys. Rev. Lett.* **2010**, *105*, 050404.

(28) Thorwart, M.; Eckel, J.; Reina, J. H.; Nalbach, P.; Weiss, S. Enhanced Quantum Entanglement in the Non-Markovian Dynamics of Biomolecular Excitons. *Chem. Phys. Lett.* **2009**, *478*, 234−237.

(29) Nalbach, P.; Eckel, J.; Thorwart, M. Quantum Coherent Biomolecular Energy Transfer with Spatially Correlated Fluctuations. *New J. Phys.* **2010**, *12*, 065043.

(30) Sahrapour, M. M.; Makri, N. Tunneling, Decoherence, And Entanglement of Two Spins Interacting with a Dissipative Bath. *J. Chem. Phys.* **2013**, *138*, 114109.

(31) Makri, N.; Makarov, D. E. Tensor Propagator for Iterative Quantum Time Evolution of Reduced Density Matrices. I. Theory. *J. Chem. Phys.* **1995**, *102*, 4600−4610.

(32) Makri, N.; Makarov, D. E. Tensor Propagator for Iterative Quantum Time Evolution of Reduced Density Matrices. Ii. Numerical Methodology. *J. Chem. Phys.* **1995**, *102*, 4611−4618.

(33) Dunkel, E. R.; Bonella, S.; Coker, D. F. Iterative Linearized Approach to Non-adiabatic Dynamics. *J. Chem. Phys.* **2008**, *129*, 114106.

(34) Huo, P.; Coker, D. F. Iterative Linearized Density Matrix Propagation for Modeling Coherent Excitation Energy Transfer in Photosynthetic Light Harvesting Systems. *J. Chem. Phys.* **2010**, *133*, 184108.

(35) Huo, P.; Coker, D. F. Influence of Environment Induced Correlation Fluctuations in Electronic Coupling on Coherent Excitation Energy Transfer Dynamics in Model Photosynthetic Systems. *J. Chem. Phys.* **2012**, *136*, 115102.

(36) Roden, J.; Eisfeld, A.; Wolff, W.; Strunz, W. T. Influence of Complex Exciton-Phonon Coupling on Optical Absorption and Energy Transfer of Quantum Aggregates. *Phys. Rev. Lett.* **2009**, *103*, 058301.

(37) Ishizaki, A.; Fleming, G. R. On the Adequacy of the Redfield Equation and Related Approaches to the Study of Quantum Dynamics in Electronic Energy Transfer. *J. Chem. Phys.* **2009**, *130*, 234110.

(38) Ishizaki, A.; Fleming, G. R. Theoretical Examination of Quantum Coherence in a Photosynthetic System at Physiological Temperature. *Proc. Natl. Acad. Sci. U.S.A.* **2009**, *106*, 17255.

(39) Tanaka, M.; Tanimura, Y. Multistate Electron Transfer Dynamics in the Condensed Phase: Exact Calculations from the Reduced Hierarchy Equations of Motion Approach. *J. Chem. Phys.* **2010**, *132*, 214502.
(40) Sakurai, A.; Tanimura, Y. Does hbar Play a Role in Multidimensional Spectroscopy? Reduced Hierarchy Equations of Motion Approach to Molecular Vibrations. *J. Phys. Chem. A* **2011**, *115*, 4009−4022.
(41) Jang, S.; Cheng, Y. C.; Reichman, D. R.; Eaves, J. D. Theory of Coherent Resonance Energy Transfer. *J. Chem. Phys.* **2008**, *129*, 101104.
(42) Jang, S. Theory of Coherent Resonance Energy Transfer for Coherent Initial Condition. *J. Chem. Phys.* **2009**, *131*, 164101.
(43) Nazir, A. Correlation-Dependent Coherent to Incoherent Transitions in Resonant Energy Transfer Dynamics. *Phys. Rev. Lett.* **2009**, *103*, 146404.
(44) McCutcheon, D. P. S.; Nazir, A. Coherent and Incoherent Dynamics in Excitonic Energy Transfer: Correlated Fluctuations and off-Resonance Effects. *Phys. Rev. B* **2011**, *83*, 165101.
(45) Chen, Q. H.; Zhang, Y. Y.; Liu, T.; Wang, K. L. Numerically Exact Solution to the Finite-Size Dicke Model. *Phys. Rev. A* **2008**, *78*, 051801.
(46) Zhao, Y.; Zanardi, P.; Chen, G. H. Quantum Entanglement and the Self-Trapping Transition in Polaronic Systems. *Phys. Rev. B* **2004**, *70*, 195113.
(47) Breuer, H.-P.; Petruccione, F. *The Theory of Open Quantum Systems*; Oxford University Press: New York, 2002.
(48) Renyi, A. *Proceedings of the Fourth Berkeley Symposium on Mathematical Statistics and Probability 1960*; University of California Press: Berkeley, 1961.
(49) Lü, Z. G.; Zheng, H. Non-Markovian Dynamical Effects and Time Evolution of the Entanglement Entropy of a Dissipative Two-State System. *Europhys. Lett.* **2009**, *86*, 60009.
(50) Sarovar, M.; Ishizaki, A.; Fleming, G. R.; Whaley, K. B. Quantum Entanglement in Photosynthetic Light-Harvesting Complexes. *Nat. Phys.* **2010**, *6*, 462−467.
(51) Dijkstra, A. G.; Tanimura, Y. Non-Markovian Entanglement Dynamics in the Presence of System-Bath Coherence. *Phys. Rev. Lett.* **2010**, *104*, 250401.
(52) Zhang, Y. Y.; Duan, L. W.; Chen, Q. H.; Zhao, Y. Polaronic Discontinuities Induced by off-Diagonal Coupling. *J. Chem. Phys.* **2012**, *137*, 034108.
(53) Zhao, Y.; Chernyak, V.; Mukamel, S. Spin versus Boson Baths in Nonlinear Spectroscopy. *J. Phys. Chem. A* **1998**, *102*, 6614−6634.
(54) Shenai, P.; Chernyak, V.; Zhao, Y. Disorder Influenced Absorption Line Shapes of a Chromophore Coupled to Two-Level Systems. *J. Phys. Chem. A* **2013**, *117*, 12320−12331.
(55) Förster, T. Transfer Mechanisms of Electronic Excitation. *Discuss. Faraday Soc.* **1959**, *27*, 7−17.
(56) Dexter, D. L. A Theory of Sensitized Luminescence in Solids. *J. Chem. Phys.* **1953**, *21*, 836−850.